Asymmetric and Independent Contribution of the Second Transmembrane Segment 12′ Residues to Diliganded Gating of Acetylcholine Receptor Channels

A Single-Channel Study with Choline as the Agonist

Claudio Grosman and Anthony Auerbach

From the Department of Physiology and Biophysics, State University of New York at Buffalo, Buffalo, New York 14214

abstract Mutagenesis studies have suggested that the second transmembrane segment (M2) plays a critical role during acetylcholine receptor liganded gating. An adequate description of the relationship between gating and structure of the M2 domain, however, has been hampered by the fact that many M2 mutations increase the opening rate constant to levels that, in the presence of acetylcholine, are unresolvably fast. Here, we show that the use of saturating concentrations of choline, a low-efficacy agonist, is a convenient tool to circumvent this problem. In the presence of 20 mM choline: (a) single-channel currents occur in clusters; (b) fast blockade by choline itself reduces the single-channel conductance by ~50%, yet the excess open-channel noise is only moderate; (c) the kinetics of gating are fitted best by a single-step, C ↔ O model; and (d) opening and closing rate constants are within a well resolvable range. Application of this method to a series of recombinant adult mouse muscle M2 12′ mutants revealed that: (a) the five homologous M2 12′ positions make independent and asymmetric contributions to diliganded gating, the δ subunit being the most sensitive to mutation; (b) mutations at δ12′ increase the diliganded gating equilibrium constant in a manner that is consistent with the sensitivity of the transition state to mutation being ~30% like that of the open state and ~70% like that of the closed state; (c) the relationship between δ12′ amino acid residue volume, hydrophobicity or α-helical tendency, and the gating equilibrium constant of the corresponding mutants is not straightforward; however, (d) rate and equilibrium constants for the mutant series are linearly correlated (on log–log plots), which suggests that the conformational rearrangements upon mutation are mostly local and that the position of the transition state along the gating reaction coordinate is unaffected by these mutations.

key words: nicotinic receptors • allosteric proteins • Brønsted plot • kinetics • double-mutant cycles

INTRODUCTION

The four transmembrane segments (M1–M4)[1] of the acetylcholine receptor (AChR) are likely to be involved in the conformational changes associated with gating (Filatov and White, 1995; Labarca et al., 1995; Ohno et al., 1995; Unwin, 1995; Campos-Caro et al., 1997; Wang et al., 1997, 1999; Bouzat et al., 1998; Chen and Auerbach, 1998; Tamamizu et al., 1999). However, because the lining of the pore (Akabas et al., 1994; Zhang and Karlin, 1998), the gate (Wilson and Karlin, 1998), and the size- (Villarroel et al., 1991; Cohen et al., 1992) and charge-selectivity filters (Galzi et al., 1992; Corringer et al., 1999) are basically contributed by residues of M2, this transmembrane segment is particularly important.

An adequate description of the relationship between function and structure of the M2 segment has been hampered by the fact that many mutations increase the channel opening rate constant ("gain-of-function" mutations). The opening rate constant of wild-type AChRs, in the presence of ACh, is at the upper limit of reliable estimation (~30,000–100,000 s^{-1}; Maconochie and Steinbach, 1998), thus even a modest increase makes this parameter too fast to be resolved. As a consequence, many groups have described the effects of M2 mutations in terms of aggregate parameters such as the observed open times of single-channel currents, or the EC_{50} of a whole-cell dose–response curve. Unfortunately, these are compound parameters that are determined by a combination of binding and gating processes and therefore provide limited information about the role of M2 in channel opening and closing per se. This explains why, despite the wealth of data that is available on M2 mutants, the understanding of how M2 residues participate in the control of gating has progressed slowly. Although most M2 mutations increase the duration of observed openings and lower the EC_{50},

Address correspondence to Claudio Grosman, Department of Physiology and Biophysics, School of Medicine and Biomedical Sciences, SUNY at Buffalo, 124 Sherman Hall, Buffalo, NY, 14214. Fax: 716-829-2569; E-mail: grosman@buffalo.edu

[1]*Abbreviations used in this paper:* AChR, acetylcholine channel; LFER, rate-equilibrium linear free-energy relationship; M2, second transmembrane segment; rms, root mean square.

J. Gen. Physiol. © The Rockefeller University Press • 0022-1295/2000/05/637/15 $5.00
Volume 115 May 2000 637–651
http://www.jgp.org/cgi/content/full/115/5/637

it has been difficult to attribute these effects to changes in specific rate constants.

One way of dealing with this limitation is to work with a slowly opening mutant on the background of which the mutations of interest are engineered. This approach was taken by Chen and Auerbach (1998), who used the αD200N mutant, a binding-site mutant with a reduced opening rate constant, as the background AChR on which M2 mutations were introduced. Here we used an alternative method: clusters of openings were elicited with 20 mM choline, a "slowly opening," low-efficacy agonist (Zhou et al., 1999). With this approach, most of the closed sojourns were detected, and the complexity of the closed-time distribution was reduced to a single exponential density.

We applied this method to investigate the contribution of the M2 12′ residues of the four different AChR subunits (a Ser in δ and a Thr in α, β, and ϵ) to gating. By dissecting the effects of mutations on either the opening or the closing rate constant, we provide a detailed picture of the relationship between structure and gating in this region of M2. The results indicate that these positions contribute in an independent and asymmetrical manner to gating, which is most affected by mutations in the δ subunit. They also suggest that there is a complex relationship between gating and the physicochemical properties of the amino acid residue in δ12′, and that the increase in gating equilibrium constant upon mutation is mostly due to a decrease in the closing rate constant with a smaller contribution of an increase in the opening rate constant. For δ 12′ mutations, the logarithms of the rate and equilibrium constants of gating are linearly correlated with a slope that suggests that the local environment of this M2 position is ∼30% open-like (70% closed-like) at the transition state of the gating conformational change.

METHODS

Expression, Electrophysiology, and Kinetic Modeling

Mouse AChR cDNA clones, transient expression in HEK-293 cells, cell-attached patch-clamp recordings, cluster definition in the presence of saturating concentrations of agonist, and kinetic analysis were as described in the preceding paper (Grosman and Auerbach, 2000). δS268T and ϵT264S mutations were engineered by overlap PCR (Higuchi, 1990). For all other mutations, the QuikChange™ Site-Directed Mutagenesis Kit (Stratagene, Inc.) protocol was followed. All constructs were confirmed by dideoxy sequencing.

Error Estimates

Standard errors of the calculated (as opposed to experimentally determined) variables in Tables III and IV, say $Y = f(X_i)$, were estimated according to the following expressions:

$$Var(Y) = \sum_{i=1}^{n}\left[\left(\frac{\partial Y}{\partial X_i}\right)^2 \cdot Var(X_i)\right] \quad (1)$$

and

$$Var(Y) = SE^2(Y); \qquad Var(X_i) = SE^2(X_i), \quad (2)$$

where $\partial Y/\partial X_i$ is the partial derivative of Y with respect to each random variable (X_i) evaluated at the corresponding experimentally derived mean values, $Var(X_i)$ is the variance of X_i, and n is the number of different X_i variables. Eq. 1 assumes that the random variables are uncorrelated (i.e., that the covariance between any given pair of X_i is zero) and it is exact only when Y is a linear function of X_i. When $Y(X_i)$ is a nonlinear function (our case in Tables III and IV), the result is only approximate because it is the variance of only the linear portion of the Taylor power-series expansion of $Y(X_i)$. However, the smaller the values of $Var(X_i)$, the more accurate the approximation.

Open-Channel Noise

The experimental excess open-channel noise was calculated by subtracting the closed-level variance from the open-level variance, and is expressed as the ratio between the standard deviation (root mean square, rms) of the noise (σ_{ex}) and the single-channel current amplitude (i). Such variances were calculated directly from the digitized currents once the samples ("points") were sorted into the closed and open "classes" by the idealization procedure. Thermal (σ_{th}) and shot (σ_{sh}) excess noise were calculated by Eq. 3 (Horowitz and Hill, 1980):

$$\sigma_{th} = \sqrt{4k_B T\gamma B}, \quad (3)$$

where k_B is Boltzmann's constant, T is the absolute temperature (∼295°K), γ is the single-channel conductance, and B is the bandwidth, and (Eq. 4):

$$\sigma_{sh} = \sqrt{2iqB}, \quad (4)$$

where q is the elementary charge (1.602×10^{-19} coulomb). The sum of these two sources of excess noise was calculated by adding their variances, and it is expressed as a standard deviation.

Coupling Energies

Coupling energies between mutations (see Table III) were calculated as:

$$\Delta G^{o} = -RT\ln\frac{\theta_x\theta_y}{\theta_B\theta_{x+y}}, \quad (5)$$

where R is the universal gas constant, and the θ values are the diliganded gating equilibrium constants (the ratio between the opening and closing rate constants) of the background receptor (B), the single mutants (x and y), and the double mutant (x + y). Values calculated in this way are referred to as "mean" values. The corresponding standard errors were calculated by applying Eqs. 1 and 2 to Eq. 5.

From Eq. 5 it can be seen that if mutational effects were additive (i.e., if $\Delta G^{o} = 0$):

$$\theta_B\theta_{x+y} = \theta_x\theta_y. \quad (6)$$

This expression was used to calculate the expected diliganded gating equilibrium constant values (θ_2) of double mutants (see Table III) or the wild type (see Table IV), given the θ_2 values of the other three members of the cycle.

Coefficients of variation (see Table III) were calculated as:

$$C_v = \frac{\Delta\theta}{\theta_{observed}}, \quad (7)$$

where $\Delta\theta$ is the difference between the observed ($\theta_{observed}$) and the calculated (from Eq. 6) values of θ_2 for the double mutants.

RESULTS

Choline as an Agonist

Fig. 1 A shows continuous single-channel traces of 12′ δS→T AChRs in the presence of a saturating concentration (20 mM) of choline. At this concentration, openings occurred in clusters separated by long-lived silent periods. As with openings elicited by ACh, each cluster represents the activity of a single channel, and the silent intervals between them correspond to sojourns in desensitized states (Sakmann et al., 1980). Clusters were defined so that the intracluster closed intervals were monoexponentially distributed (Fig. 1 B). The openings within clusters turned out to follow a monoexponential distribution as well, a fact that is in marked contrast with the multiexponential nature of openings of M2 12′ mutants in the absence of ligand (Grosman and Auerbach, 2000). The kinetics of AChR activity in the presence of 20 mM choline were thus reduced to those of the C ↔ O reaction scheme. Fig. 2 shows the mean open and closed times, on a cluster-by-cluster basis, for seven patches containing the 12′ δS→T mutant.

One consequence of working with high concentrations of cholinergic agonists is the occurrence of fast blockade. Due to this phenomenon, the current amplitude is reduced and the excess open-channel noise is increased. With respect to the amplitude decrease, both 20 mM choline and 2 mM ACh reduced the current amplitude of δS→T receptors by ∼50% (3.2 pA at approximately −100 mV). The current amplitude in the presence of blocker (i_B) is given by Eq. 8:

$$i_B = \frac{i_o}{1 + \frac{[B]}{K_B}}, \quad (8)$$

where i_o is the current in the absence of blocker, [B] is the blocker's concentration, and K_B is its dissociation equilibrium constant from the pore-blocking site. Therefore, K_B is ∼20 mM for choline and ∼2 mM for ACh (Auerbach and Akk, 1998) at approximately −100 mV.

Although the effect of 20 mM choline and 2 mM ACh on the current amplitude was approximately the same, the magnitude of the open-channel noise was different for these two agonists (Fig. 3). The excess open-channel noise of δS→T AChR in the presence of 20 mM choline (σ_{ex} = 0.560 pA; i = 3.4 pA) was less than one third that in the presence of 2 mM ACh (σ_{ex} = 1.818 pA; i = 3.4 pA), and comparable with that in the presence of 5 μM ACh (σ_{ex} = 0.606 pA; i = 7.4 pA), measured at the analysis bandwidth of 18 kHz. The lower noise in the presence of 20 mM choline is most likely due to the faster dissociation of choline from the blocking site.

The excess noise, expressed as a fraction of the single-channel current amplitude (σ_{ex}/i), for the wild type and all the mutants studied here is listed in Table I. Mu-

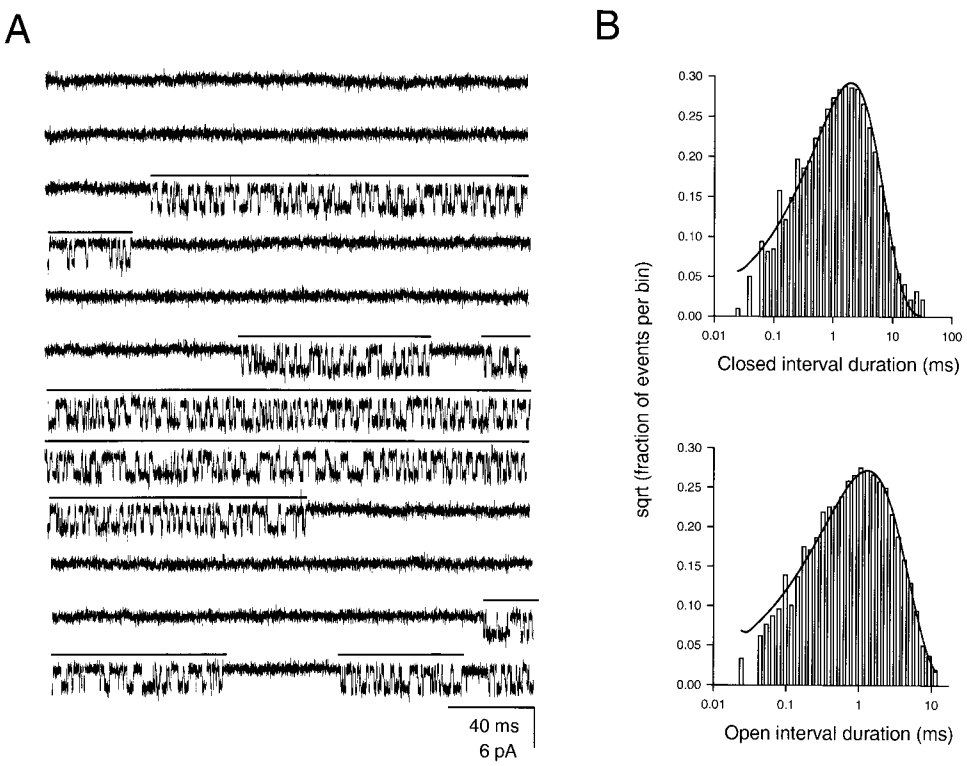

Figure 1. 12′ δS→T AChR currents in the presence of 20 mM choline. (A) Continuous single-channel traces recorded in the cell-attached configuration with 20 mM choline in the patch pipette at approximately −100 mV. For display purposes, $f_c \cong 6$ kHz. Openings are downward deflections. The solid horizontal bars indicate clusters of openings. (B) Monoexponential dwell-time histograms and superimposed density functions.

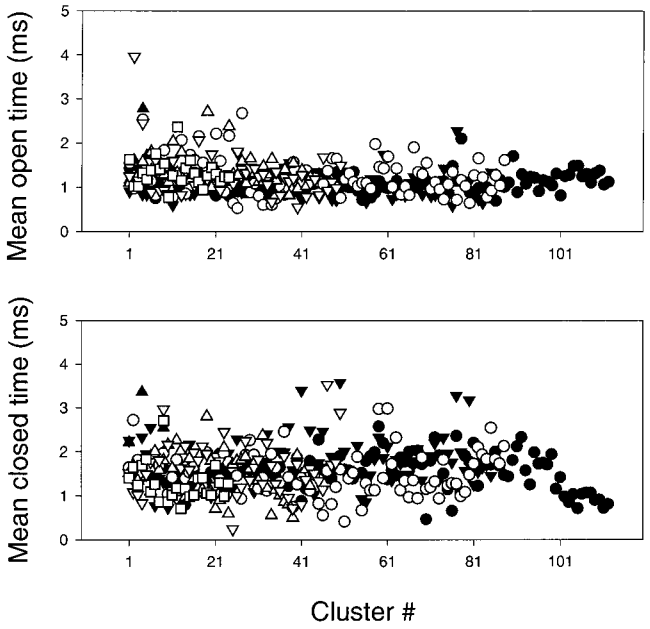

Figure 2. Mean open and closed times of 12′ δS→T AChRs in the presence of 20 mM choline. The mean of observed open and closed dwell times were calculated for 411 clusters from seven patches. A total of 38,385 openings and closings were analyzed. Each symbol identifies a different patch. Overall mean open and closed times for the seven patches were, respectively (mean ± SD, ms): 1.10 ± 0.21 and 1.54 ± 0.40, 1.57 ± 0.49 and 2.03 ± 0.62, 1.05 ± 0.28 and 1.72 ± 0.56, 1.24 ± 0.43 and 1.52 ± 0.50, 1.38 ± 0.35 and 1.51 ± 0.51, 1.28 ± 0.52 and 1.58 ± 0.60, and 1.33 ± 0.32 and 1.29 ± 0.42. Only those clusters having a mean open time within ± 2 SD of the overall mean of the corresponding patch were selected for further analysis.

tations did not substantially affect the magnitude of the excess noise. Also, during the process of cluster definition, we could not detect any additional fast component in the closed-time distribution that could have been attributed to dwellings in the blocked state. In summary, fast blockade by 20 mM choline neither affected the closed-time distributions nor significantly compromised the single-channel signal idealization process.

Since blocking events were not detected as discrete dwellings in the zero-current level, the idealized open dwell times include sojourns in both the open and blocked states. The mean duration of these apparent openings (τ) is given by:

$$\tau = \frac{K_B + [B]}{\alpha K_B + \alpha_B [B]}, \quad (9)$$

where α and α_B are the closing rate constants of the unblocked and blocked channel, respectively. In our particular case, we showed above that $K_B \cong [B]$ and, therefore, Eq. 9 reduces to Eq. 10:

$$\tau \cong \frac{2}{\alpha + \alpha_B}. \quad (10)$$

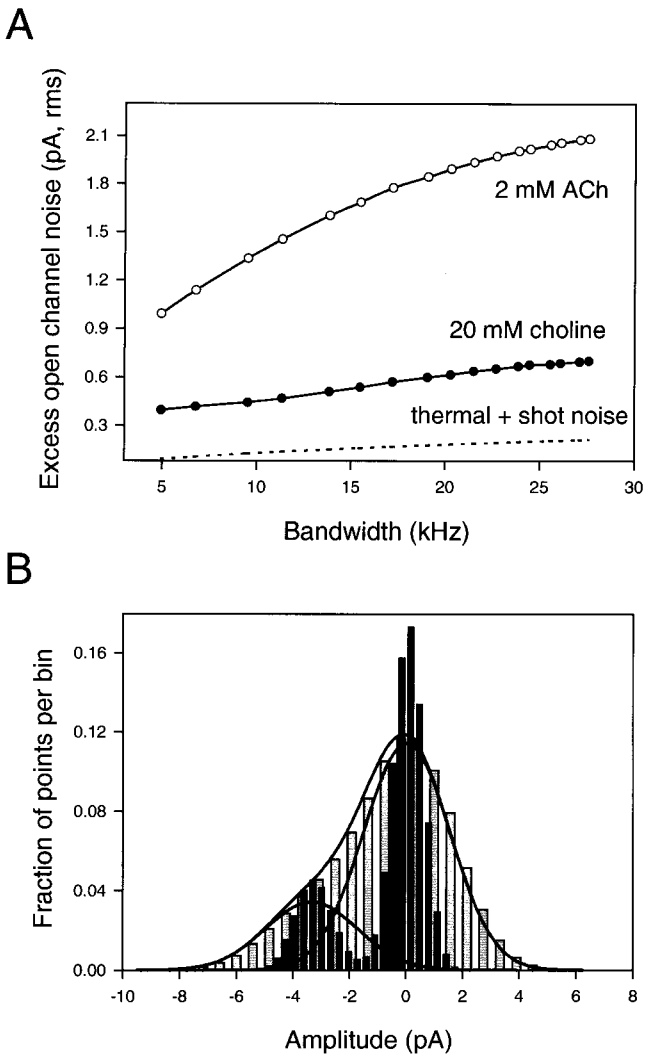

Figure 3. Noise characteristics of 12′ δS→T AChRs. (A) Excess open-channel noise (rms) of δS→T receptors activated by 20 mM choline and 2 mM ACh as a function of bandwidth. The thermal and shot noise contribution expected from an AChR activated by 20 mM choline at approximately −100 mV was calculated, and it is indicated by the dotted line. (B) All-point current-amplitude histograms of the currents in Fig. 1. (Grey bars) Histogram of data filtered at ~18 kHz (analysis bandwidth). (Black bars) Histogram of data filtered at ~6 kHz (display bandwidth). The mean and standard deviation were calculated directly from the digitized currents after idealization. These parameters were used to compute the Gaussian density functions (solid lines), an example of which is shown superimposed on the 18-kHz histogram for both the individual components and their sum.

If blocked channels could not close (i.e., $\alpha_B = 0$), then the mean duration of apparent openings would be twice as long as that of true openings in the absence of block ($1/\alpha$). This is the usual assumption, and corresponds to the sequential scheme for blockade ($C \leftrightarrow CA \leftrightarrow CA_2 \leftrightarrow OA_2 \leftrightarrow OA_2B$; Ruff, 1977; Neher and Steinbach, 1978; Sine and Steinbach, 1984; Colquhoun and Ogden, 1988; Wang et al., 1999). If, instead, channel

TABLE I

Excess Open-Channel Noise in Wild-Type and M2 12′ Mutant AChRs

AChR (S↔T combinations)	σ_{ex}/i	AChR (Different side chains)	σ_{ex}/I
Wild type (5 μM ACh)	0.104	δS→A	0.163
Wild type (2 mM ACh)	0.591	δS→G	0.183
Wild type (20 mM choline)	0.155	δS→P	0.132
αT→S	0.137	δS→W	0.240
βT→S	0.183	δS→C	0.192
ϵT→S	0.162	δS→T (5 μM ACh)	0.082
αT→S + βT→S	0.174	δS→T (2 mM ACh)	0.520
αT→S + δS→T	0.210	δS→T (20 mM choline)	0.166
αT→S + ϵT→S	0.111	δS→I	0.178
βT→S + δS→T	0.187	δS→Y	0.190
βT→S + ϵT→S	0.169	δS→V	0.189
δS→T + ϵT→S	0.173	δS→N	0.140
βT→S + δS→T + ϵT→S	0.161	δS→Q	0.225
αT→S + βT→S + δS→T + ϵT→S	0.192	δS→K	0.234

σ_{ex}/i ratios were calculated as indicated in methods in the presence of 20 mM choline, unless otherwise indicated. The contribution from thermal and shot noise was not subtracted from the excess open-channel rms noise. The membrane potential was approximately −100 mV and $f_c \cong 18$ kHz.

closings were oblivious to the presence of blocker (i.e., $\alpha_B = \alpha$), then the mean duration of openings in the presence or absence of block would be the same. It has been shown that muscle AChRs can close while blocked by QX-222 (Neher, 1983) or the ganglionic nicotinic blocker chlorisondamine (Neely and Lingle, 1986). Therefore, assuming that the blocker cannot speed the channel's closure, our closing rate-constant estimates are underestimated by a factor ≤2. As no obvious differences between constructs were observed in the single-channel amplitude reduction, we conclude that K_B is similar for all of them and, hence, that all the closing rate constant were underestimated by the same factor.

Effects of 12′ S→T and T→S Mutations

The probability of being open within a cluster of diliganded openings was higher in δS→T AChRs than in the wild type because the unliganded gating equilibrium constant increases with the mutation (Grosman and Auerbach, 2000). Fig. 4 shows single-channel clusters of the wild type and a set of 12′ mutants in the presence of 20 mM choline, displayed in increasing order of number of mutated subunits. The mutations were S→T in δ and T→S in α, β, and ϵ subunits. Table II shows the results of the kinetic analysis.

Gating is most affected by mutations in δ. Mutations in β and ϵ increase the diliganded gating equilibrium constant (θ_2) to a smaller extent but while the former increases the opening rate and decreases the closing rate, the latter increases both rate constants. A more detailed analysis of this difference in kinetics will be given below. Mutations in both α subunits result in a minor reduction in the gating equilibrium constant. This effect is more evident when the mutation is engineered on a background receptor that has a higher θ_2. The addition of the αT→S mutation to constructs having a single mutation in either the β, δ, or ϵ subunit yields receptors with somewhat lower θ_2 values. This effect is even clearer when the β + δ + ϵ mutant combi-

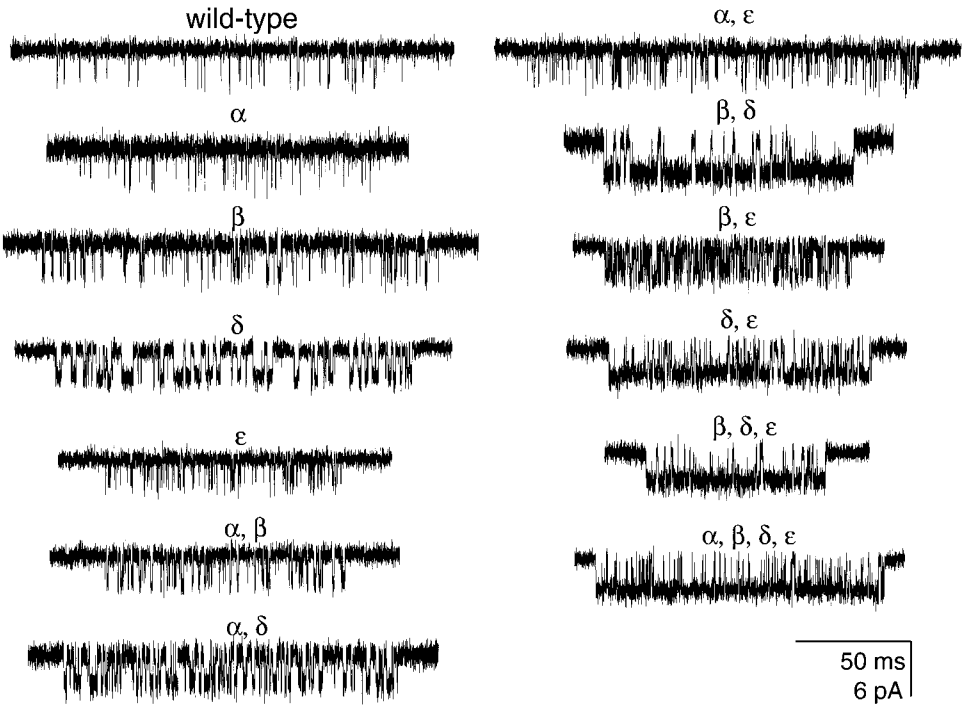

Figure 4. Single-channel clusters of wild-type AChRs and receptors having S→T and T→S mutations in M2 12′. Membrane potential ≅ −100 mV. Display $f_c \cong 6$ kHz. Openings are downwards.

TABLE II

Effects of 12′ S→T and T→S Mutations on the Kinetic and Equilibrium Parameters of Gating in 20 mM Choline

AChR	12′ residue				Rates		θ_2		No. patches	No. clusters	No. intervals
	α	β	δ	ϵ	β_2	α_2	Mean	SEM			
					s^{-1}	s^{-1}					
Wild type	T	T	S	T	257	4954	0.054	0.010	5	193	14015
αT254S	S	T	S	T	279	6930	0.043	0.014	3	329	34462
βT265S	T	S	S	T	734	2872	0.265	0.027	6	584	47354
δS268T	T	T	T	T	667	869	0.783	0.059	7	382	36813
ϵT264S	T	T	S	S	2653	14264	0.189	0.033	3	82	12878
αT→S + βT→S	S	S	S	T	958	3665	0.264	0.047	4	111	6482
αT→S + δS→T	S	T	T	T	961	1843	0.518	0.064	4	421	33194
αT→S + ϵT→S	S	T	S	S	1342	7599	0.182	0.020	6	287	31505
βT→S + δS→T	T	S	T	T	1246	476	2.766	0.387	4	235	10257
βT→S + ϵT→S	T	S	S	S	4386	4226	1.062	0.082	4	174	19422
δS→T + ϵT→S	T	T	T	S	2767	972	2.782	0.218	6	296	43614
βT→S + δS→T + ϵT→S	T	S	T	S	4738	375	12.688	0.597	4	167	4900
αT→S + βT→S + δS→T + ϵT→S	S	S	T	S	6755	730	9.410	0.822	3	110	5100

The opening (β_2) and closing (α_2) rate constants were estimated by using a maximum-likelihood algorithm that includes a correction for missed events (program MIL; Qin et al., 1996, 1997). Their mean values for the indicated number of patches are shown. Because of channel block, the α_2 values were underestimated by a factor ≤2. This factor is approximately the same for all the constructs (see results). Currents were idealized at an 18-kHz bandwidth (program SKM). Membrane potential was approximately −100 mV. θ_2 mean values were calculated by averaging the β_2/α_2 ratios of individual patches, not as the ratio between the means of these two rate constants. The number of intervals includes both closed and open sojourns in the idealized dwell-time series after imposing a fixed resolution ("dead time"). The dead time varied from patch to patch, and the average was ∼29 μs.

nation with and without the mutation in α is compared. Thus, the effect of mutations in the α subunits (a slight decrease in θ_2) differs qualitatively from those of mutations in the other subunits (an increase in θ_2).

If the effect of a given mutation is independent of the background receptor, as hinted above, then the effects of the multiple mutations should be additive (Wells, 1990; Dill, 1997). Deviations from additivity can be quantified by comparing predicted (as if single mutations acted independently) versus observed θ_2 values, and calculating the corresponding coupling energies (Eq. 5). These can be calculated for any pair of mutations by designing double-mutant thermodynamic cycles (Carter et al., 1984). Fig. 5 shows all possible cycles (using the S→T and T→S constructs studied here) that test for deviations from independence between pairs of single mutations. Table III gives estimates of such deviations calculated as coefficients of variation (Eqs. 6 and 7) and as free energies of coupling (Eq. 5). The small magnitude of the latter suggests that the effects of the different mutations on the equilibrium properties of mutant AChRs can be considered to be essentially additive. Indeed, in the context of allosteric transitions and protein folding, values of $\Delta G^{o}_{coupling} < 0.2$ kcal/mol are considered negligible (Carter et al., 1984; Hurle et al., 1986; Perry et al., 1989; Aharoni and Horovitz, 1997). An alternative way of displaying the close proximity between the predicted and observed equilibrium properties of M2 12′ mutants is shown in Fig. 6. Additivity of mutational effects occurs whenever: (a) there are no pairwise interactions between the tested residues in either the closed or the open conformation, (b) pairwise interactions exist but they do not change upon gating, or (c) these pairwise interactions are not disrupted by the mutations.

Prediction of Agonist Efficacies using Double-Mutant Cycles

Finding regions of a protein that make independent contributions to function is a powerful tool in protein engineering. The right combination of single-point mutations necessary to modify a given function to a desired extent can be chosen to tailor a multiply mutated protein based on the behavior of the single mutants. In our case, we found that this approach can be used to expand the variety of chemical structures that can be examined in agonist structure–function relation studies. For example, when bound to wild-type AChRs, choline is such a low-efficacy agonist that clusters are hard to define and, therefore, the ability to estimate θ_2 is compromised. However, choline's efficacy (θ_2) is easily measured when bound to M2 12′ mutants. Because any combination of T→S and S→T mutations at the M2 12′ position have additive effects (Figs. 4 and 5, and Table III), the efficacy of choline on the wild type could be predicted based on the θ_2 values of choline on mutant receptors. Fig. 7 shows all the double-mutant cycles, having the wild type in one of the vertices, that can be formed with the set of mutations in Table II. In each case, the efficacy of choline on the wild type was as-

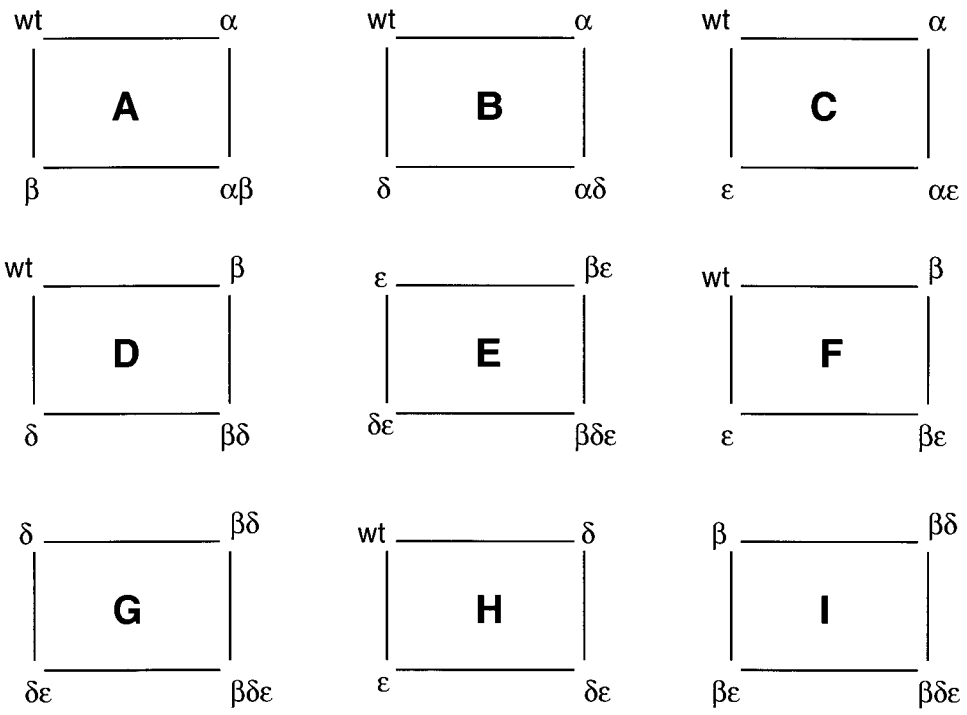

Figure 5. Double-mutant cycles. Nine cycles designed to investigate the additivity of mutational effects in M2 12′. "αβ," for example, denotes the double mutant αT→S + βT→S.

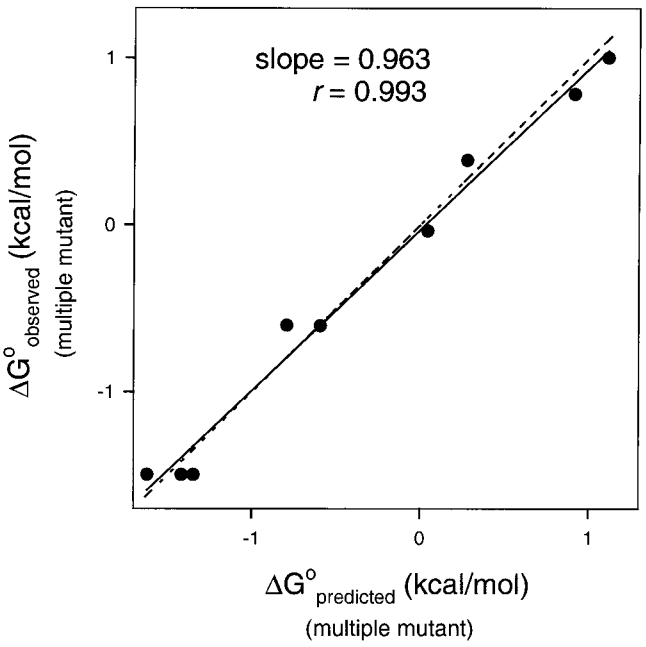

Figure 6. Plot showing the correlation between calculated ("predicted") and experimentally derived ("observed") ΔG^{o} values ($-RT \ln\theta_2$) for the nine multiple mutants in Fig. 5 (e.g., αβ in cycle A, βδε in cycle E). θ_2 values were calculated by assuming additivity (Eq. 6). The solid line is the fit to a straight line. The dashed line has unity slope and $r = 1$; i.e., it represents the ideal situation of complete independence between mutations. The close agreement between both straight lines suggests that deviations from additivity, if any, are small.

sumed to be unknown and was calculated according to Eq. 6. The values calculated from the 13 cycles and their average are listed in Table IV along with the average of experimentally determined efficacies. The fact that these two values are almost identical confirms the experimental value of θ_2 for choline on the wild type (∼0.05) and suggests the applicability of this protein-engineering approach to other very-low-efficacy agonists.

Since the closing rate constant values were underestimated (because of fast blockade), the θ_2 values dis-

TABLE III

Additivity of Mutational Effects

Mutant cycle	Pairwise interaction tested	Coefficient of variation	$\Delta G^{o}_{coupling}$ Mean	$\Delta G^{o}_{coupling}$ SEM
			kcal/mol	
A	α–β	0.200	0.132	0.251
B	α–δ	0.204	−0.110	0.236
C	α–ϵ	0.173	0.112	0.252
D	β–δ	0.390	−0.193	0.156
E	β–δ	0.232	−0.123	0.125
F	β–ϵ	0.127	0.080	0.168
G	β–ϵ	0.225	0.150	0.108
H	δ–ϵ	0.015	0.009	0.163
I	δ–ϵ	0.126	0.080	0.115

Coefficients of variation were calculated according to Eq. 7. Coupling free-energy changes ($\Delta G^{o}_{coupling}$) were calculated according to Eq. 5. It is important to emphasize here that the standard errors of the $\Delta G^{o}_{coupling}$ values were calculated (Eqs. 1 and 2) by assuming that the mutations are independent. Therefore, the SEM should be taken with caution when deciding whether the mutational effects are additive or not.

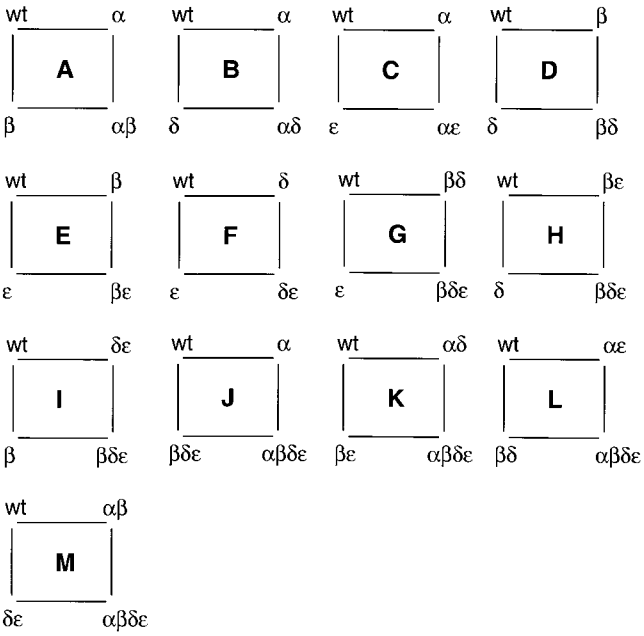

Figure 7. Double-mutant cycles. Thirteen cycles designed to predict choline's efficacy on wild-type receptors based on the concept of additivity of mutational effects.

played throughout this paper should not be taken as absolute efficacies of choline on the various constructs. The ratios between these values, however, should be good estimates of the choline's relative efficacies.

Contribution of the δ12′ Position to Gating

The results in Fig. 4 and Table II indicate that the S→T mutation in δ has a greater effect on the equilibrium properties of gating than T→S changes in the other subunits. In an attempt to better understand the structural basis of the role of the δ12′ position during gating, different amino acid residues were substituted by site-directed mutagenesis. Fig. 8 shows single-channel clusters of the wild type and a set of δ12′ mutants in the presence of 20 mM choline, displayed in increasing order of θ_2. The results of the kinetic analysis are displayed in Table V and show that, as θ_2 increases, the closing rate constant decreases and the opening rate constant increases, although to a smaller extent (Fig. 9).

Fig. 10 plots log θ_2 (a measure of the free-energy change upon gating) against some properties of the substituted amino acids. As far as the volume is concerned, in the range between ~60 and 150 Å^3, the bulkier a residue, the larger is θ_2. However, this general trend is lost above ~160 Å^3 (i.e., for Ile, Tyr, and Trp). With respect to hydrophobicity, highly hydrophilic residues such as Lys, Gln, and Asn have the largest θ_2 values. However, among less hydrophilic residues, this parameter is not correlated with θ_2. A lack of correlation was also found between θ_2 and the α helical propensity, both in polar and nonpolar environments, of the δ12′ residues. We conclude that the relationship between the gating equilibrium constant of δ12′ mutant channels and the physicochemical properties of the mutated residues is complex.

TABLE IV

Prediction of the Efficacy of Choline on Wild-Type AChRs

	Predicted wild-type θ_2 value	
Mutant	Mean	SEM
A	0.043	0.017
B	0.065	0.023
C	0.045	0.017
D	0.075	0.014
E	0.047	0.010
F	0.053	0.011
G	0.041	0.009
H	0.066	0.008
I	0.058	0.008
J	0.058	0.020
K	0.058	0.010
L	0.053	0.011
M	0.078	0.017

Average of predicted θ_2 values, 0.057 ± 0.012 (mean ± SEM); average of experimentally determined θ_2 values, 0.054 ± 0.010 (mean ± SEM). The θ_2 value of wild-type receptors bound to choline was calculated from the efficacies of choline on single and double-mutants based on the finding that 12′ mutations are independent (Table III). If the efficacy of choline on the wild type is assumed to be unknown, only the mutant cycles E, G, and I (Fig. 5) should be considered to test for independence of mutational effects. Analysis of these three cycles indicate that the M2 12′ mutations in the β–δ, β–ϵ, and δ–ϵ subunit pairs act independently. Since α_2 values are affected by block, so are the θ_2 values.

Linear-free Energy Relationships

In contrast with the complexity noted above, Fig. 9 reveals a very regular relation between kinetics and equilibrium in δ12′ mutants. As the gating equilibrium constant increases, the opening rate constant increases, and the closing rate constant decreases almost monotonically. This type of behavior, which is not demanded by any law of thermodynamics, is usually referred to as an "extrathermodynamic" relationship (Leffler and Grunwald, 1963). Such relations are most conveniently displayed on a log–log scale (Fig. 11 A, equivalent to a $\Delta G^{\ddagger}$-vs.-ΔG^{o} plot), where the points are fitted best with a straight line. This type of plot is common in physical organic chemistry and is known as a "Brønsted plot" (Brønsted and Pedersen, 1924), while the relation between the activation and the equilibrium free-energy changes is best known as a "rate-equilibrium linear free-energy relationship" (LFER; Leffler and Grunwald, 1963). The fact that this relation is linear firmly suggests that the relative position of the gating transition state along the reaction coordinate does not change upon mutation (Grosman et al., 2000). This, in

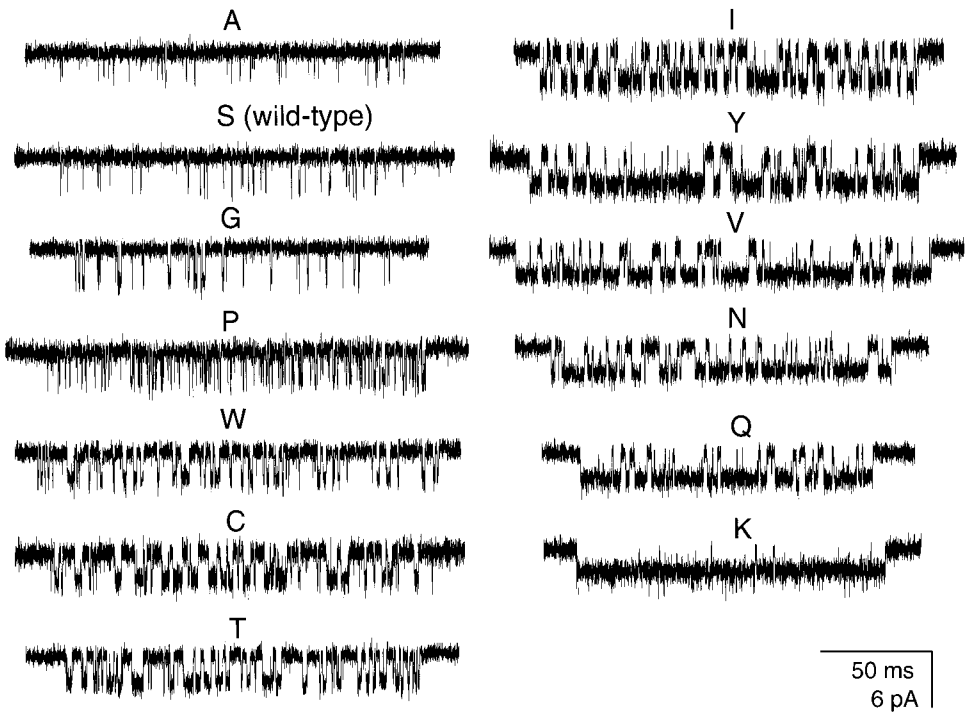

Figure 8. Single-channel clusters of wild-type AChRs and a series of δ12′ mutants. Membrane potential ≅ −100 mV. Display f_c ≅ 6 kHz. Openings are downwards.

turn, suggests that the conformational perturbations caused by the different side-chain substitutions are graded versions of the same local rearrangement.

The Brønsted relationship can be written as:

$$\log\beta_2 = \Phi\log\theta_2 + \text{constant}, \qquad (11)$$

where Φ, the slope, reflects the relative position of the local environment of the mutated residue along the reaction pathway at the time that the transition state is reached. Therefore, Φ ranges from 0 (closed-like) to 1 (open-like). An analogous expression holds for α_2, the slope being (Φ − 1). It is remarkable that the linearity of this relationship holds for a three-order-of-magnitude range of θ_2 values (from ∼0.035 in δS→A to ∼35 in δS→K). As show in Fig. 11 A, at δ12′, Φ = 0.275 ± 0.023.

There has been some debate as to the statistical validity of a Brønsted plot (log k vs. log k/k') as a measure of

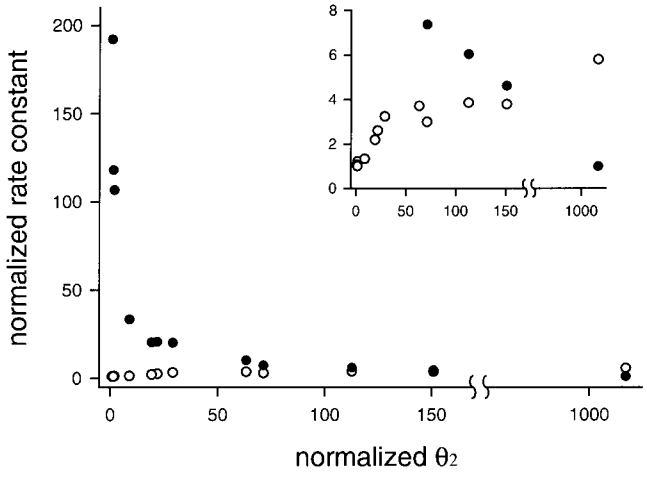

Figure 9. Gating rate constants versus gating equilibrium constants. (●) α_2 vs. θ_2, (○) β_2 vs. θ_2. The axes are normalized to their respective smallest values. The inset emphasizes the smaller but significant increase in the opening rate constant, β_2. The points correspond to all the different residues tested in δ12′, with the exception of Pro.

TABLE V

Effects of Different Amino Acids in the δ12′ Position on the Kinetic and Equilibrium Parameters of Gating in 20 mM Choline

δ12′ residue	Rates		θ_2		No. patches	No. clusters	No. intervals
	β_2	α_2	Mean	SEM			
	s^{-1}	s^{-1}					
A	272	8059	0.035	0.007	3	76	11180
S (wild type)	257	4954	0.054	0.010	5	193	14015
G	312	4476	0.069	0.003	3	52	6172
P	948	3952	0.242	0.034	3	70	15758
W	342	1398	0.313	0.101	3	52	4102
C	560	856	0.671	0.076	6	328	46934
T	667	869	0.783	0.059	7	382	36813
I	830	846	1.011	0.088	7	346	28726
Y	951	432	2.200	0.208	5	77	2990
V	766	309	2.478	0.345	2	21	975
N	989	253	3.911	0.146	6	144	6019
Q	971	194	5.236	0.594	4	214	4602
K	1489	42	35.272	2.522	2	282	2176

See legend to Table II for details. The average dead time was ∼39 μs.

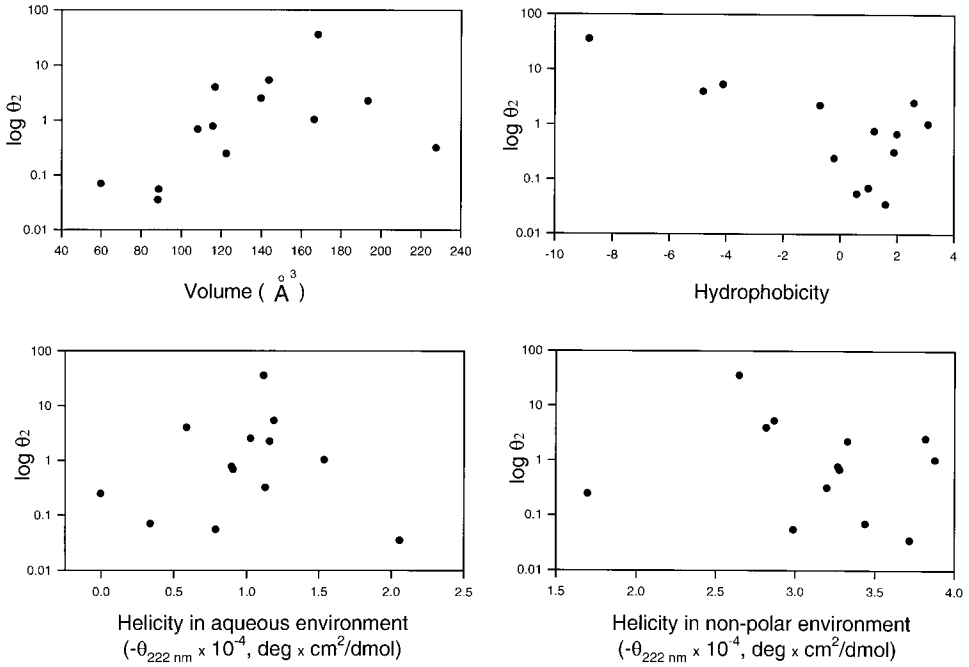

Figure 10. θ_2 values of δ12′ mutants and corresponding physicochemical properties of the mutant residues. The relationship between amino acid residue volume (Zamyatnin, 1972), hydrophobicity (Engelman, Steitz, and Goldman scale; Branden and Tooze, 1991), or α-helical tendency (Liu and Deber, 1998) and the gating equilibrium constant of δ12′ mutants is not straightforward.

the existence of a linear relation (Estell, 1987). It has been concluded that a double-logarithmic plot of the rate constants (log k vs. log k') is a more stringent statistical test (Fersht, 1987). Rearranging Eq. 11 gives Eq. 12:

$$\log\beta_2 = \frac{\Phi}{\Phi - 1}\log\alpha_2 + \text{constant}'. \qquad (12)$$

Fig. 11 B shows such a plot for the δ12′ mutant series. From this plot, we estimate that $\Phi = 0.268 \pm 0.022$, which is very close to the value estimated from the Brønsted plot. We conclude that, at the transition state of diliganded gating, the interactions of the δ12′ position with the rest of the protein are 27% like those in the open state and 73% like those in the closed state.

The solid lines in Fig. 11, A and B, are the results of the linear regressions through all the data points (●), with the exception of that corresponding to the δS→P mutant (◇). The behavior of this mutant was considered to be an outlier based on the analysis shown in Table VI. The different behavior of the Pro mutant is also evident from a cursory examination of the data in Table V. The increase in β_2 upon the S→P mutation is ∼ 3.4-fold larger than the one expected from the observed 1.25-fold decrease in α_2 and a Φ-value of 0.275.

We can go back now to Table II and analyze the S→T and T→S mutations from an LFER perspective. The δS→T mutant is a member of the mutant series plotted in Fig. 11. As compared with the wild type, opening is faster and closing is slower in this mutant, as expected from a mutation that alters the stability of the transition state to an extent that is intermediate between the effects on the stability of the ground (closed and open) states. The slope, Φ, between δS→T and the wild type (only considering these two points) is ∼0.357. The mutation βT→S also increases the opening rate and decreases the closing rate, but the slope between this mutant and the wild type is $\Phi = 0.663$. This suggests that the transition state has a more open-like character (i.e., the stabilization of the transition state follows that of the open state more closely) at β12′ than at δ12′. Although more mutations are needed to confirm the different slope of β12′, the different values of Φ suggest that the movement of the β subunit precedes that of the δ subunit during the opening reaction.

TABLE VI

Correlation Coefficients for Different Data Sets

Data set	Correlation coefficient (r)	Data set	Correlation coefficient (r)
All mutants	0.816	−T	0.816
−A	0.772	−I	0.824
−S	0.789	−Y	0.813
−G	0.792	−V	0.816
−P	0.945	−N	0.805
−W	0.833	−Q	0.805
−C	0.818	−K	0.763

The correlation coefficients between log β_2 and log α_2 were calculated (SigmaPlot, Version 3.01; Jandel Scientific) for different data sets. "−X" means that the data point corresponding to the residue X was omitted from the data set. The number of data points are 13 ("all mutants") or 12 ("−X"). Omission of P increases r to a considerable extent. Therefore, the behavior of the δS→P AChR was considered to be an outlier.

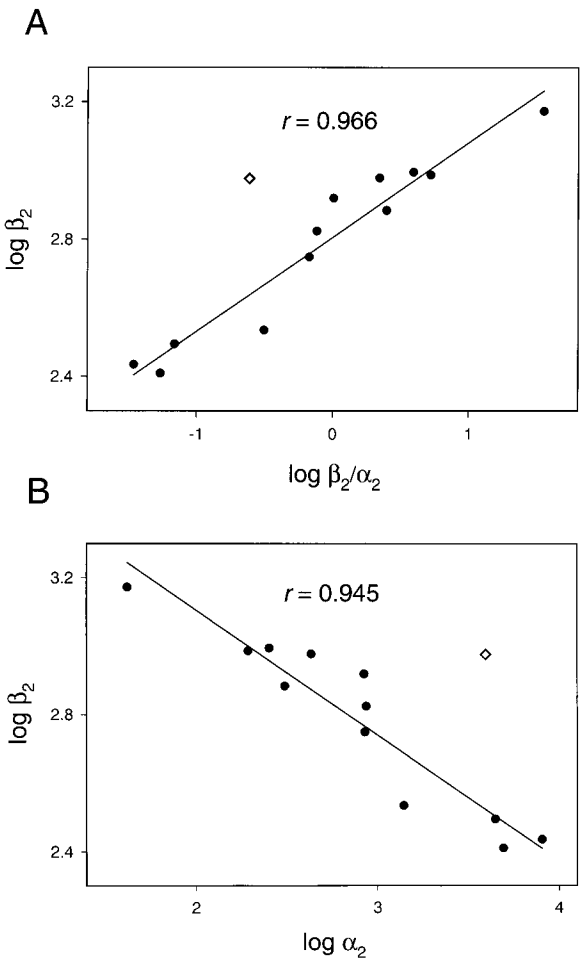

Figure 11. Two different ways of displaying a rate-equilibrium LFER. (A) Brønsted plot. The slope (Φ) is 0.275 ± 0.023. The slope of such plots is most commonly denoted as "β" or "α," after Brønsted's work (Brønsted and Pedersen, 1924). In our case, to avoid confusion with the AChR subunits (α, β, δ, ϵ) or the diliganded gating rate constants (β_2, α_2), we adopted the letter "Φ," after Fersht's application of the LFER concept to protein folding (e.g., Fersht, 1994). (B) log *k* vs. log *k*′ plot. The slope [$\Phi/(\Phi - 1)$] is −0.366 ± 0.040 and, therefore, Φ is 0.268 ± 0.022. The two Φ values do not exactly coincide because the values of θ_2 in A are not the ratios between the y and x axis values in B, but the average of θ_2 values across patches (see Table II, legend). Solid lines in A and B are least-square fits to straight lines of the data corresponding to all the different residues tested in δ12′ (●) with the exception of Pro (◇). *r*, correlation coefficients. On a logarithmic scale, the underestimation of α_2 values is manifest as an offset and, therefore, does not affect the slope estimates.

Free-Energy Relationships Are Not Always Linear

The T→S perturbation in the ϵ subunit alters the behavior of the channel in a different manner than when engineered in the β or the δ subunit. In this case, both opening and closing rate constants get faster and, thus, an LFER does not hold. Therefore, this mutation has a "catalytic" effect stabilizing the transition state to a greater extent than either ground state. In qualitative terms, this effect of the ϵT→S mutation is also observed when the mutation is engineered on other background AChRs (αT→S, βT→S, or δS→T; Table II). Regardless of the background receptor, the increase in the opening rate is far more pronounced than the increase in the closing rate.

The effect of the αT→S mutation (in both subunits) on the kinetics of gating is more difficult to assess because, like its effect on the equilibrium constant (see above), the changes were modest. Nevertheless, when coexpressed with other mutant subunits, this effect becomes evident. On the background of the single mutants βT→S or δS→T, or of the triple mutant βT→S + δS→T + ϵT→S, the α mutation also increases both rate constants (Table II). This suggests that the slightly larger values of the opening and closing rate constants of αT→S receptors, as compared with the wild type, represent genuine changes as well. It is interesting to note that the αT→S mutation does not increase the rates of the ϵT→S mutant when both mutations are coexpressed. This contrasts with the results in Table III, which show that the effects of these two mutations on θ_2 are additive. If the effects of the αT→S and ϵT→S mutations on the rate constants had been additive as well, the opening and closing rate of the double mutant would have been 2,880 and 19,953 s^{-1}, respectively (from Eq. 6, replacing equilibrium constants with rate constants). As compared with the effect of the T→S mutation in the ϵ subunit (the other "catalytic" mutation), the T→S substitution in α affects the opening and closing rate constants to a smaller and more even extent.

DISCUSSION

Choline as an Agonist: An Alternative Approach

Extracting rate constants from single-channel data can be difficult. The observed open and closed interval durations are often related in a complex way with the underlying rate constants, which can only be estimated through the application of elaborate algorithms (for example, Colquhoun and Hawkes, 1981; Horn and Lange, 1983; Qin et al., 1996, 1997). In addition, when the data become scarce, the ability of these techniques to estimate the correct rate constants necessarily decreases. This is what happens, for example, with many M2 mutants. Due to the increased opening rate constant, and given the instrumental limitations, dwellings in the closed diliganded state are severely underrepresented in the idealized set of intervals.

The use of a saturating concentration of choline, a low-efficacy agonist that supports a slow opening rate constant, is a very useful tool to reliably estimate the gating rate constants of 12′ M2 mutants. None of the drawbacks associated with the use of a blocking concentration of agonist posed a serious problem. Instead,

most closures were detected and the kinetic complexity of the channel was reduced to that of a closed ↔ open reaction scheme.

It was somewhat surprising that the open times followed a single exponential considering that spontaneous (Grosman and Auerbach, 2000) and ACh-elicited (Ohno et al., 1995; Chen and Auerbach, 1998) openings of certain 12′ mutants require two to three components to be fitted correctly. Even though multiple exponential components in the open-time distribution of ACh-gated currents could be accounted for by openings arising from AChRs with different degrees of ligation, those resulting from unliganded receptors cannot. For practical purposes and for the interpretation of rates in terms of energy barriers, though, having a single open state in the model was very convenient.

We envisage that this weak-agonist approach will become a useful tool to characterize the gating structure–function relationships of other regions of the receptor that, like M2 12′, increase the diliganded opening rate constant (β_2) upon mutation. Mutations that affect K_B (the dissociation equilibrium constant of the agonist from the pore-blocking site), however, could not be dealt with by this approach because the underestimation of the closing rate constant (α_2) will no longer be the same for the entire mutant series. In these cases, α_2 should be estimated at concentrations of agonist that are low enough to prevent blockade, yet high enough to minimize the occurrence of unliganded and monoliganded openings.

Additivity of Mutational Effects: Lack of Interaction between 12′ Residues

We investigated whether interactions between the five 12′-position residues change upon (and thus contribute to the free-energy change of) gating. During wild-type diliganded gating, there is a net loss of ~2.0 kcal/mol ($\theta_2 \cong 30$) in going from the closed to the open conformation, whereas during unliganded gating there is an uphill change of ~6.5 kcal/mol [$\theta_0 \cong 1.5 \times 10^{-5}$, from Grosman and Auerbach (2000), assuming 20 channels in the patch]. If the end points of the gating conformational change were the same with or without agonist bound, then the ~8.5-kcal/mol difference between unliganded and diliganded gating would be provided, in its entirety, by the excess ligand-binding energy to the open state (i.e., exclusively by agonist-receptor interactions). Nevertheless, as these ligand–protein contacts are absent during spontaneous gating, protein–protein interactions must also change (some noncovalent bonds break, others get formed) to account for the ~6.5-kcal/mol increase in the free energy of the unliganded open AChR as compared with the unliganded closed form. Moreover, it is likely that these same changes in protein–protein contacts will occur upon liganded gating as well.

While considerable progress has been made in identifying the amino acid residues that interact with the agonist at the transmitter binding sites (reviewed in Hucho et al., 1996), very little (if any) is known about the protein–protein contribution to the overall free-energy balance of gating. We investigated the existence of such interactions by comparing the θ_2 values of various constructs in the context of a double-mutant cycle analysis (Carter et al., 1984). The effects of S→T (in δ) and T→S (elsewhere) 12′ mutations on θ_2 turned out to be additive (Table III). Also, structural data suggest that cysteines engineered in α and β 12′ do not face the lumen of the channel (Akabas et al., 1994; Zhang and Karlin, 1998, but see Machold et al., 1995 for δ12′). Taken together, we suggest that interactions between 12′ residues do not exist at all, in either the closed or open conformations of the channel and, thus, do not contribute to the ΔG^o of gating.

Additivity of Mutational Effects: Application to Agonist Structure–Function Studies

The diversity of chemical structures that can be examined in agonist structure–function relation studies is limited by the nature of the receptor used. For example, the efficacy of ACh on the wild-type receptor is so high that more efficacious ligands could hardly be identified if tested on the same receptor. Likewise, agonists with very low efficacy would elicit currents that only seldom get clustered, an absolute requirement for this type of analysis. Application of the "protein engineering" method described here should significantly broaden the range of molecules that can be analyzed in these structure–function studies. By selecting the right combination of independent mutations, the efficacy of virtually any molecule on the wild type could be known. Here, we showed how this approach was used in the case of choline, an agonist of very low efficacy on muscle AChRs. A similar procedure, engineering additive mutations that slow channel opening, could be applied to test for ligands with higher efficacy than ACh.

Structural Aspects of the 12′ Position

The M2 12′ position is very well conserved among the members of the superfamily of nicotinoid receptors (see first table in Grosman and Auerbach, 2000) being most commonly a Thr and, more rarely, a Ser or an Ala. In muscle AChRs, this position is occupied by Thr in α, β, ε/γ, and a Ser in δ.

From a physicochemical viewpoint, S→T and T→S mutations are rather subtle substitutions. Nevertheless, the asymmetry of the muscle AChR's M2 12′ position is very well conserved across species, even though only a

single-nucleotide mutation is needed to turn the δ12′ Ser (TCT) into a Thr, or the α (ACC) or β/ϵ/γ (ACT) 12′ Thr into a Ser. It was interesting then to test the functional effects of S→T and T→S mutations.

The results in this paper indicate that even these conservative mutations affect gating, δ being the most sensitive and α the least sensitive subunit (even less considering that both α subunits were mutated). In addition, we showed that the three constructs having Ser only in α, β, or ϵ subunits (Thr elsewhere) have θ_2 values that are ∼10-, ∼51-, and ∼52-fold higher than the wild-type's value. In the context of synaptic transmission, these receptors would give rise to slowly decaying endplate currents much like congenital myasthenic-syndrome mutants do (assuming that the mutations do not affect the kinetics of agonist dissociation). Therefore, there seems to be a tight requirement for a single Ser in 12′ for normal function, and this Ser has to be in δ. With respect to different side chains in δ12′, only an S→A or S→G mutation would still be compatible with normal synaptic transmission.

The marked functional asymmetry of this ring of residues leads us to propose that the 12′ positions of the different subunits face different environments. This would be the case if, for example, the orientation of the M2 α helices around the central pore differed between subunits. Alternatively, this could also happen if the five M2 12′ positions, having the same orientation, were packed against the transmembrane segments M1/M3, whose amino acid sequences vary from subunit to subunit.

The relationship between θ_2 and several physicochemical properties of the residue occupying δ12′ is not straightforward, at least when these properties are considered one at a time, as in Fig. 10. However, the response to volume and hydrophobicity can, to some extent, be rationalized in the framework of the 12′ residues being packed against M1 (Akabas et al., 1994) and/or M3 in a tight and hydrophobic environment. It is interesting to note that both Ser and Thr display a higher tendency to occur in membrane-embedded α helices than in aqueous-based ones (Liu and Deber, 1998). This is, at least in part, because the hydrogen-bonding capacity of the Ser and Thr hydroxyl groups can be satisfied by participating in bifurcated intrachain hydrogen bonds with the carbonyl oxygen in the preceding turn of the same α helix (MacKenzie et al., 1997). As far as the kinetic and equilibrium properties of gating are concerned, however, the relevance of the hydrogen-bonding capacity of Ser seems to be minimal, as suggested by the small effect of the S→A mutation. We hypothesize, then, that a combination of steric hindrance and hydrophobic interactions in the local environment of δ12′ can explain the observed effects of mutations. Side chains bulkier than the $-CH_2$-OH of Ser [but no larger than the $-CH$-$(CH_3)_2$ of Val] would cause steric repulsion in both the closed and open states. However, this repulsion should be larger in the closed channel conformation to account for the net destabilization of the closed with respect to the open state (i.e., the increase in θ_2) that accompanies the mutations. This further suggests that, upon opening, there has to be an increase in the volume between δ12′ and the residue/s against which it packs to explain how an increase in the volume of the side chain causes less strain in the open than in the closed state. It is not clear why the three bulkiest residues tested (Ile, Tyr, and Trp) deviate from this trend. That side chains smaller than that of Ser, like the $-CH_3$ of Ala and the $-H$ of Gly, do not substantially decrease θ_2 suggests that the cavity where the wild-type Ser is located has the right dimensions to hold the $-CH_2$-OH side chain and that there is not much steric hindrance to be relieved.

We also observed that receptors having Lys, Asn, or Gln at δ12′ (the three more hydrophilic residues tested) displayed the largest θ_2 values. These residues are expected to weaken the hydrophobic interactions that contribute to the putative helix–helix packing in both the closed and open conformations. As these mutations increase θ_2, the packing seems to be tighter in the closed than in the open state, where a looser association of transmembrane domains might relieve the strain of having to accommodate a highly hydrophilic side chain.

In summary, both volume and hydrophobicity considerations lead us to speculate that there is an expansion in the volume around δ12′ upon channel opening.

Linear Free-Energy Relationships

The fact that mutational effects in δ 12′ conform to linear free-energy relationships is firm evidence that the tested side chains (with the probable exception of Pro) affect the structure of the AChR in a qualitatively similar way, as if the resulting structural changes were part of a continuum (Fersht et al., 1986). This may seem surprising, especially considering the disparate nature of the amino acids used in the mutagenesis, and the relatively broad range of mutational effects recorded (∼1,000-fold increase in θ_2). Nevertheless, single point mutations usually cause only local rearrangements (Skinner and Terwilliger, 1996), and a three-order-of-magnitude change in an equilibrium constant corresponds to only ∼4 kcal/mol. It is likely that much larger variations in θ_2 are needed to observe the predicted deviations from linearity (Hammond, 1955; Leffler and Grunwald, 1963; Mok and Polanyi, 1969) that arise when not only the height but also the shape of the barrier changes. It is also likely that these θ_2 values would be too extreme to be estimated correctly and, therefore, that most LFER applications to gating will be in the linear range.

It is not at all obvious that an LFER should always hold. Such relations are only expected to occur for positions in the protein where the change in the transition state's free energy upon mutation is the linear combination of the free-energy changes of the ground states (Leffler, 1953; Leffler and Grunwald, 1963; Fersht et al., 1986; Grosman et al., 2000). In fact, AChRs having the T→S substitution in α or ϵ deviate from such behavior, suggesting that these mutations affect local interactions of the α and ϵ 12′ sidechains that are present only at the transition state. As a consequence, the position of the α and ϵ 12′ residues along the reaction coordinate of gating cannot be revealed by the LFER approach, at least when a T→S mutation is used as the perturbation.

As mentioned earlier, the behavior of the δS→P receptor was also anomalous. With our results so far, it is not possible to assert that the reason why this mutant is an outlier (Fig. 11 and Table VI) lies on the proline's different backbone properties (Pro can act as a hydrogen-bond acceptor but not as a donor). To unequivocally address this issue, the wild-type Ser should be replaced with its corresponding α-hydroxi acid (glyceric acid) so as to preserve the side chain while changing the hydrogen-bonding pattern to that of Pro. This can be done by resorting to the use of unnatural amino acid mutagenesis (England et al., 1999). However, even in the absence of such unnatural-mutation data, the fact that the side chain of Pro does not have any remarkable peculiarity leads us to speculate that the intrachain α-helix hydrogen bonds contributed by M2 δ12′ play an important role during the process of gating.

We thank Karen Lau for technical assistance.

This work was supported by grants from the National Institutes of Health to A. Auerbach and from the American Heart Association, New York State Affiliate, to C. Grosman.

Submitted: 24 September 1999
Revised: 3 March 2000
Accepted: 20 March 2000

REFERENCES

Aharoni, A., and A. Horovitz. 1997. Detection of changes in pairwise interactions during allosteric transitions: coupling between local and global conformational changes in GroEL. *Proc. Natl. Acad. Sci. USA.* 94:1698–1702.

Akabas, M.H., C. Kaufmann, P. Archdeacon, and A. Karlin. 1994. Identification of acetylcholine receptor channel-lining residues in the entire M2 segment of the α subunit. *Neuron.* 13:919–927.

Auerbach, A., and G. Akk. 1998. Desensitization of mouse nicotinic acetylcholine receptor channels. A two gate mechanism. *J. Gen. Physiol.* 112:181–197.

Bouzat, C., A.M. Roccamo, I. Garbus, and F.J. Barrantes. 1998. Mutations at lipid-exposed residues of the acetylcholine receptor affect its gating kinetics. *Mol. Pharmacol.* 54:146–153.

Branden, C., and J. Tooze. 1991. Introduction to Protein Structure. Garland Publishing, Inc., New York, NY. 210 pp.

Brønsted, J.N., and K. Pedersen. 1924. Die katalytische Zersetzung des Nitramids und ihre physikalisch-chemische Bedeutung. *Z. Phys. Chem.* 108:185–235.

Campos-Caro, A., J.C. Rovira, F. Vicente-Agulló, J.J. Ballesta, S. Sala, M. Criado, and F. Sala. 1997. Role of the putative transmembrane segment M3 in gating of neuronal nicotinic receptors. *Biochemistry.* 36:2709–2715.

Carter, P.J., G. Winter, A.J. Wilkinson, and A.R. Fersht. 1984. The use of double mutants to detect structural changes in the active site of the tyrosyl-tRNA synthetase (*Bacillus stearothermophilus*). *Cell.* 38:835–840.

Chen, J., and A. Auerbach. 1998. A distinct contribution of the δ subunit to acetylcholine receptor channel activation revealed by mutations of the M2 segment. *Biophys. J.* 75:218–225.

Cohen, B.N., C. Labarca, L. Czyzyk, N. Davidson, and H.A. Lester. 1992. $Tris^+/Na^+$ permeability ratios of nicotinic acetylcholine receptors are reduced by mutations near the intracellular end of the M2 region. *J. Gen. Physiol.* 99:545–572.

Colquhoun, D., and G.A. Hawkes. 1981. On the stochastic properties of single ion channels. *Proc. R. Soc. Lond. B Biol. Sci.* 211:205–235.

Colquhoun, D., and D.C. Ogden. 1988. Activation of ion channels in the frog end-plate by high concentrations of acetylcholine. *J. Physiol.* 395:131–159.

Corringer, P.J., S. Bertrand, J.L. Galzi, A. Devillers-Thiéry, J.P. Changeux, and D. Bertrand. 1999. Mutational analysis of the charge selectivity filter of the α7 nicotinic acetylcholine receptor. *Neuron.* 22:831–843.

Dill, K.A. 1997. Additivity principles in biochemistry. *J. Biol. Chem.* 272:701–704.

England, P.M., Y. Zhang, D.A. Dougherty, and H.A. Lester. 1999. Backbone mutations in transmembrane domains of a ligand-gated ion channel: implications for the mechanism of gating. *Cell.* 96:89–98.

Estell, D.A. 1987. Artifacts in the application of linear free-energy analysis. *Prot. Eng.* 1:441–442.

Fersht, A.R. 1987. Linear free-energy relationships are valid! *Prot. Eng.* 1:442–445.

Fersht, A.R. 1994. Characterizing transition states in protein folding: an essential step in the puzzle. *Curr. Opin. Struct. Biol.* 5:79–84.

Fersht, A.R., R.J. Leatherbarrow, and T.N.C. Wells. 1986. Quantitative analysis of structure-activity relationships in engineered proteins by linear free-energy relationships. *Nature.* 322:284–286.

Filatov, G.N., and M.M. White. 1995. The role of conserved leucines in the M2 domain of the acetylcholine receptor in channel gating. *Mol. Pharmacol.* 48:379–384.

Galzi, J.L., A. Devillers-Thiéry, N. Hussy, S. Bertrand, J.P. Changeux, and D. Bertrand. 1992. Mutations in the channel domain of a neuronal nicotinic receptor convert ion selectivity from cationic to anionic. *Nature.* 359:500–505.

Grosman, C., and A. Auerbach. 2000. Kinetic, mechanistic, and structural aspects of unliganded gating of acetylcholine receptor channels: a single-channel study of second transmembrane segment 12′ mutants. *J. Gen. Physiol.* 115:621–635.

Grosman, C., M. Zhou, and A. Auerbach. 2000. Mapping the conformational wave of acetylcholine receptor channel gating. *Nature.* 403:773–776.

Hammond, G.S. 1955. A correlation of reaction rates. *J. Am. Chem. Soc.* 77:334–338.

Higuchi, R. 1990. Recombinant PCR. *In* PCR Protocols. A Guide to Methods and Applications. M.A. Innis, D.H. Gelfand, J.J. Sninsky, and T.J. White, editors. Academic Press, Inc., San Diego, CA. 177–183.

Horn, R., and K. Lange. 1983. Estimating kinetic constants from single channel data. *Biophys. J.* 43:207–223.

Horowitz, P., and W. Hill. 1980. The art of electronics. Cambridge

University Press, New York, NY. 288–289.

Hucho, F., V.I. Tsetlin, and J. Machold. 1996. The emerging three dimensional structure of a receptor. The nicotinic acetylcholine receptor. *Eur. J. Biochem.* 239:539–557.

Hurle, M.R., N.B. Tweedy, and C.R. Matthews. 1986. Synergism in folding of a double mutant of the α subunit of tryptophan synthase. *Biochemistry.* 25:6356–6360.

Labarca, C., M.W. Nowak, H. Zhang, L. Tang, P. Deshpande, and H.A. Lester. 1995. Channel gating governed symmetrically by conserved leucine residues in the M2 domain of nicotinic receptors. *Nature.* 376:514–516.

Leffler, J.E. 1953. Parameters for the description of transition states. *Science.* 117:340–341.

Leffler, J.E., and E. Grunwald. 1963. Rates and equilibria of organic reactions. John Wiley & Sons, New York, NY. 458 pp.

Liu, L.-P., and C.M. Deber. 1998. Uncoupling hydrophobicity and helicity in transmembrane segments. *J. Biol. Chem.* 273:23645–23648.

Machold, J., Y. Utkin, D. Kirsch, R. Kaufmann, V. Tsetlin, and F. Hucho. 1995. Photolabeling reveals the proximity of the α-neurotoxin binding site to the M2 helix of the ion channel in the nicotinic acetylcholine receptor. *Proc. Natl. Acad. Sci. USA.* 92:7282–7286.

MacKenzie, K.R., J.H. Prestegard, and D.M. Engelman. 1997. A transmembrane helix dimer: structure and implications. *Science.* 276:131–133.

Maconochie, D.J., and J.H. Steinbach. 1998. The channel opening rate of adult- and fetal-type mouse muscle nicotinic receptors activated by acetylcholine. *J. Physiol.* 506:53–72.

Mok, M.H., and J.C. Polanyi. 1969. Location of energy barriers. II. Correlation with barrier height. *J. Chem. Phys.* 51:1451–1469.

Neely, A., and C.J. Lingle. 1986. Trapping of an open-channel blocker at the frog neuromuscular acetylcholine channel. *Biophys. J.* 50:981–986.

Neher, E. 1983. The charge carried by single-channel currents of rat cultured muscle cells in the presence of local anesthetics. *J. Physiol.* 339:663–678.

Neher, E., and J.H. Steinbach. 1978. Local anesthetics transiently block currents through single acetylcholine-receptor channels. *J. Physiol.* 277:153–176.

Ohno, K., D.O. Hutchinson, M. Milone, J.M. Brengman, C. Bouzat, S.M. Sine, and A.G. Engel. 1995. Congenital myasthenic syndrome caused by prolonged acetylcholine receptor channel openings due to a mutation in the M2 domain of the ϵ subunit. *Proc. Natl. Acad. Sci. USA.* 92:758–762.

Perry, K.M., J.J. Onuffer, M.S. Gittelman, L. Barmat, and C.R. Matthews. 1989. Long-range electrostatic interactions can influence the folding, stability, and cooperativity of dihydrofolate reductase. *Biochemistry.* 28:7961–7968.

Qin, F., A. Auerbach, and F. Sachs. 1996. Estimating single-channel kinetic parameters from idealized patch-clamp data containing missed events. *Biophys. J.* 70:264–280.

Qin, F., A. Auerbach, and F. Sachs. 1997. Maximum likelihood estimation of aggregated Markov processes. *Proc. R. Soc. Lond. B Biol. Sci.* 264:375–383.

Ruff, R.L. 1977. A quantitative analysis of local anesthetic alteration of miniature end-plate currents and end-plate current fluctuations. *J. Physiol.* 264:89–124.

Sakmann, B., J. Patlak, and E. Neher. 1980. Single acetylcholine-activated channels show burst-kinetics in presence of desensitizing concentrations of agonist. *Nature.* 286:71–73.

Sine, S.M., and J.H. Steinbach. 1984. Agonists block currents through acetylcholine receptor channels. *Biophys. J.* 46:277–284.

Skinner, M.M., and T.C. Terwilliger. 1996. Potential use of additivity of mutational effects in simplifying protein engineering. *Proc. Natl. Acad. Sci. USA.* 93:10753–10757.

Tamamizu, S., Y.-H. Lee, B. Hung, M.G. McNamee, and J.A. Lasalde-Dominicci. 1999. Alteration in ion channel function of mouse nicotinic acetylcholine receptor by mutations in the M4 transmembrane domain. *J. Membr. Biol.* 170:157–164.

Unwin, N. 1995. Acetylcholine receptor channel imaged in the open state. *Nature.* 373:37–43.

Villarroel, A., S. Herlitze, M. Koenen, and B. Sakmann. 1991. Location of a threonine residue in the α-subunit M2 transmembrane segment that determines the ion flow through the acetylcholine receptor channel. *Proc. R. Soc. Lond. B Biol. Sci.* 243:69–74.

Wang, H.-L., A. Auerbach, N. Bren, K. Ohno, A.G. Engel, and S.M. Sine. 1997. Mutation in the M1 domain of the acetylcholine receptor α subunit decreases the rate of agonist dissociation. *J. Gen. Physiol.* 109:757–766.

Wang, H.-L., M. Milone, K. Ohno, X.-M. Shen, A. Tsujino, A.P. Battochi, P. Tonali, J. Brengman, A.G. Engel, and S.M. Sine. 1999. Acetylcholine receptor M3 domain: stereochemical and volume contributions to channel gating. *Nat. Neurosci.* 2:226–233.

Wells, J.A. 1990. Additivity of mutational effects in proteins. *Biochemistry.* 37:8509–8517.

Wilson, G.G., and A. Karlin. 1998. The location of the gate in the acetylcholine receptor channel. *Neuron.* 20:1269–1281.

Zamyatnin, A.A. 1972. Protein volume in solution. *Prog. Biophys. Mol. Biol.* 24:109–123.

Zhang, H., and A. Karlin. 1998. Contribution of the β subunit M2 segment to the ion-conducting pathway of the acetylcholine receptor. *Biochemistry.* 37:7952–7964.

Zhou, N., A.G. Engel, and A. Auerbach. 1999. Serum choline activates mutant acetylcholine receptors that cause slow channel congenital myasthenic syndromes. *Proc. Natl. Acad. Sci. USA.* 96: 10466–10471.